Received: 28 November 2020 | Revised: 6 April 2021 | Accepted: 9 April 2021

DOI: 10.1111/cas.14921

ORIGINAL ARTICLE

Cancer Science WILEY

Suppression of lysosomal acid alpha-glucosidase impacts the modulation of transcription factor EB translocation in pancreatic cancer

Ryoga Hamura[1,2] | Yoshihiro Shirai[1,2] | Yohta Shimada[2] | Nobuhiro Saito[1,2] | Tomohiko Taniai[1,2] | Takashi Horiuchi[1,2] | Naoki Takada[1,2] | Yumi Kanegae[3] | Toru Ikegami[1] | Toya Ohashi[2] | Katsuhiko Yanaga[1]

[1]Department of Surgery, Jikei University School of Medicine, Tokyo, Japan

[2]Division of Gene Therapy, Research Center for Medical Science, Jikei University School of Medicine, Tokyo, Japan

[3]Core Research Facilities of Basic Science, Research Center for Medical Science, Jikei University School of Medicine, Tokyo, Japan

Correspondence
Yoshihiro Shirai, Jikei University School of Medicine, 3-25-8, Nishi-Shinbashi, Minato-ku, Tokyo 105-8461, Japan.
Email: shirai@jikei.ac.jp

Funding information
Japan Society for the Promotion of Science (JSPS) KAKENHI Grant, Grant/Award Number: 17K16584, 20K17665; The Jikei University Research Fund; Uehara Memorial Foundation Research Incentive Grant

Abstract

Lysosomal degradation plays a crucial role in the metabolism of biological macromolecules supplied by autophagy. The regulation of the autophagy-lysosome system, which contributes to intracellular homeostasis, chemoresistance, and tumor progression, has recently been revealed as a promising therapeutic approach for pancreatic cancer (PC). However, the details of lysosomal catabolic function in PC cells have not been fully elucidated. In this study, we show evidence that suppression of acid alpha-glucosidase (GAA), one of the lysosomal enzymes, improves chemosensitivity and exerts apoptotic effects on PC cells through the disturbance of expression of the transcription factor EB. The levels of lysosomal enzyme were elevated by gemcitabine in PC cells. In particular, the levels of GAA were responsive to gemcitabine in a dose–dependent and time–dependent manner. Small interfering RNA against the *GAA* gene (si*GAA*) suppressed cell proliferation and promoted apoptosis in gemcitabine-treated PC cells. In untreated PC cells, we observed accumulation of depolarized mitochondria. Gene therapy using adenoviral vectors carrying shRNA against the *GAA* gene increased the number of apoptotic cells and decreased the tumor growth in xenograft model mice. These results indicate that GAA is one of the key targets to improve the efficacy of gemcitabine and develop novel therapies for PC.

KEYWORDS

GAA, gene therapy, lysosome, pancreatic cancer, TFEB translocation

1 | INTRODUCTION

Intracellular nutrient metabolism is accelerated in cancer cells because of the rapid cell proliferation and high requirement of substrate for anabolism. Macroautophagy (termed autophagy) refers to the adaptation of metabolic requirements in eukaryotic cells, including cancer cells.[1,2] The important roles of autophagy for proliferation, invasion, metastasis, and resistance to chemotherapy were recently demonstrated in several types of cancer cells.[2,3] Modulation of autophagy by RNA interference or small molecules (including chloroquine) enhances sensitivity to

chemotherapeutic drugs in several cancers, including pancreatic cancer (PC).[4-7] In addition, in PC cells, transcriptional control of the high expression levels of microphthalmia/transcription factor E family proteins, including transcription factor EB (TFEB) (an initiator of autophagy), regulates cancer progression and inhibition of tumor growth.[4] Therefore, regulation of autophagy is a promising approach for the development of novel therapies for PC. However, because autophagy is essential for maintaining intracellular homeostasis in human cells, its complete inhibition appears to be cytotoxic in cancer cells as well as normal cells.[8]

Autophagy is the lysosome-dependent degradation machinery for cytoplasmic components, completed by the formation of autolysosomes that are composed of autophagosomes with lysosomes. Clearance of autophagosomes is dependent on the function of lysosomal enzymes, which include more than 50 acidic hydrolases (eg, glycosidases, proteases, and sulfatases).[9] Each lysosomal enzyme has unique substrate specificity and activity. Genetic defects related to the synthesis of the enzymes induce different types of lysosomal storage diseases accompanied by accumulation of autophagosomes.[10] Although lysosomal enzymes appear to be promising targets for the modulation of autophagy, the detailed role of each enzyme in homeostasis in cancer cells remains unclear.

Recently, the quality control of mitochondria by autophagy, termed mitophagy, has attracted attention as one of the homeostatic roles of autophagy. Because mitochondrial function is involved in energy production and is a key factor for the control of cell apoptosis and autophagy via the BCL2 family,[11] mitophagy affects the survival of cancer cells.[12] Indeed, in cancer, mitophagy is triggered by the accumulation of damaged mitochondria and several stresses, such as the generation of reactive oxygen species (ROS), as an escape mechanism from apoptosis.[12,13] Accumulation of malfunctional mitochondria appears to be a key component of the anticancer effect of autophagic inhibition.

Lysosomal acid alpha-glucosidase (GAA), which is the causative gene of glycogen storage disease type II, catalyzes the production of glucose from glycogen in lysosomes.[14] Genetic downregulation of GAA induces storage of glycogen and accumulation of autophagic vacuoles, as well as mitochondria in skeletal muscle fiber of humans and mice.[15] Therefore, modulation of lysosomal GAA may affect cell damage and chemoresistance in PC through the accumulation of malfunctional mitochondria and autophagic dysfunction.

In this study, we aim to investigate the potential of lysosome and their enzymes in PC cells to chemosensitivity and to clarify the mechanism of the multifunctional anticancer effect of GAA suppression on PC cell lines. We also demonstrate that gene therapy using adenovirus vector (AdV) carrying shRNA (shRNA) for GAA (shGAA) is a novel promising method for the inhibition of tumor growth for PC.

2 | MATERIALS AND METHODS

2.1 | Cell lines

The human PC cell lines PANC-1 and MIA PaCa-2 were purchased from the Cell Resource Center for Biomedical Research, Institute of Development, Aging and Cancer, Tohoku University (Sendai, Japan). BxPC-3 and AsPC-1 were purchased from the American Type Culture Collection. PANC-1 and MIA PaCa-2 were maintained in DMEM (FUJIFILM Wako Pure Chemical) containing 10% FBS (Gibco) and 1% penicillin/streptomycin (Gibco). AsPc-1 and BxPC-3 were maintained in RPMI 1640 with L-glutamine (FUJIFILM Wako Pure Chemical) containing 10% FBS and 1% penicillin/streptomycin. All cell lines were cultured at 37°C with 5% CO_2.

2.2 | Reagents

Gemcitabine was purchased from Eli Lilly Japan (Kobe, Japan), dissolved in distilled water, and stored at −20°C until use. Bafilomycin A1 (B1793), 4-Methylumbelliferyl α-D-glucopyranoside (M9766) were purchased from Sigma–Aldrich.

2.3 | Antibodies

The following primary antibodies were used for western blotting. Anti–cleaved caspase 3 (CASP3; #9664), cleaved CASP8 (#9496), cleaved poly-ADP-ribose polymerase (PARP) (#9546), TFEB (#4240), lamin (#2032), and glyceraldehyde-3-phosphate dehydrogenase (#2118) were purchased from Cell Signaling Technology. GAA (ab137068), lysosomal associated membrane protein 2 (LAMP2; ab25631), and sequestosome 1 (SQSTM1)/p62 (ab56416) were purchased from Abcam. Light chain 3 (LC3; NB110-57180) was purchased from Novus Biologicals. Anti–Ki-67 antibody (MIB-1) was purchased from Dako.

2.4 | Animals

Five-week-old male nude mice (BALBc nu/nu) were purchased from CLEA Japan and housed under specific pathogen-free conditions in a biological cabinet at the Laboratory Animal Facility of the Jikei University School of Medicine. The protocol for the animal experiments was approved by the Institutional Animal Care and Use Committee of Jikei University (No. 2017-082). The studies were performed in accordance with the Guidelines for the Proper Conduct of Animal Experiments of the Science Council of Japan.

2.5 | Transmission electron microscopy

For electron microscopic observation, the cells were fixed with 2% glutaraldehyde in 0.1 M phosphate buffer overnight at 4°C and post–fixed with 1% osmium tetroxide in the same buffer at 4°C for 2 h. Dehydration was performed using a graded series of ethanol. The specimens were placed in propylene oxide in vivo and were subsequently embedded in Epok 812 (Oken). Ultrathin sections were prepared with a diamond knife, stained with uranium acetate and lead citrate, and observed using a H-7500 (Hitachi,

Tokyo, Japan) electron microscope at 80 kV. These processes were performed at the Core Research Facilities of Basic Science, Research Center for Medical Science, Jikei University School of Medicine.

2.6 | Immunofluorescent microscopy

The cells were seeded on coverslips and treated with 100 nM LysoTracker Red DND-99 (Thermo Fisher Scientific) at 37°C for 1 h followed by washing with PBS. Subsequently, the cells were incubated with 100 nM MitoTracker (Thermo Fisher Scientific) at 37°C for 30 min followed by washing with PBS. The cells were fixed using 4% paraformaldehyde (FUJIFILM Wako Pure Chemical) for 15 min at room temperature and counterstained with 4′,6-diamidino-2-phenylindole at room temperature for 5 min. Images were captured using the EVOS FL Auto 2 Imaging System (Thermo Fisher Scientific).

2.7 | Quantification of mitochondria

The fluorescence intensity was measured by flow cytometry. The cells were stained with MitoTracker at 37°C for 30 min and analyzed with an Attune NxT Flow Cytometer (Thermo Fisher Scientific).

2.8 | Microarray analysis

Total RNA was extracted from PANC-1 cells treated with gemcitabine (1 μM) for 24 h and analyzed using the Agilent 2200 TapeStation (Agilent Technology) for quality control. The expression profile of mRNA was determined using a SurePrint G3 Human GE Microarray (8×60K v3) (Agilent Technology). The experiment was performed by Cell Innovator. All microarray data have been deposited in the Gene Expression Omnibus database, with accession number GSE153460 (https://www.ncbi.nlm.nih.gov/geo/query/acc.cgi?acc=GSE153460).

2.9 | Enzyme activity

Acid alpha-glucosidase enzyme activity was assayed by 4MU α-D-glucopyranoside (Sigma–Aldrich) as previously described.[16] Protein concentration was measured using a BCA protein assay kit (Thermo Scientific). Briefly, cells were extracted with distilled water. Cell lysates were diluted with .2 mol/L phosphate-citrate buffer (pH 4.3) and incubated with 6 mmol/L 4MU α-D-glucopyranoside and 100 μmol/L acarbose (Sigma–Aldrich) at 37°C for 30 min followed by the addition of .15 mol/L glycine carbonate buffer (pH 10.4). Fluorescence intensity in samples was measured using a fluorometer RF-XXX (Shimadzu Corporation). Enzyme activity was expressed as nmol/mg protein/h.

2.10 | Western blotting

Western blotting analysis was performed as previously described[16] with minor modifications. Briefly, whole proteins from cells and tumors were extracted using 50 mM Tris-HCl pH 7.5 containing 2% sodium dodecyl sulfate, protease inhibitor cocktail, and phosphatase inhibitor cocktail (Roche). Extracted proteins were electrophoresed on 4-20% acrylamide gradient gels (Bio-Rad) in Tris-glycine buffer and transferred onto a polyvinylidene difluoride membrane using the Trans-Blot Turbo System (Bio-Rad). After blocking, the membranes were incubated with each primary antibody overnight followed by incubation with HRP-labeled secondary antibody (1:10 000 dilution, Histofine, Nichirei) for 2 h. The membranes were incubated with a luminol enhancer and peroxide solution, Clarity Max (Bio-Rad) and analyzed using a Chemi Doc XRS+ System and the Image Lab software (Bio-Rad).

2.11 | RNA interference

Gene silencing for in vitro experiments were performed using GAA-specific siRNA (siGAA). siGAA were obtained as siGENOME SMART pool (M-008881-2-0005) from GE Healthcare Dharmacon. The non–targeting siRNA control (siScr) was also obtained as siGENOME Non–Targeting siRNA Pool #1 (D-001206-13-20). The cells were transfected with siRNA using Lipofectamine RNAiMAX Reagent (Invitrogen) according to the instructions provided by the manufacturer. The knockdown effects of GAA were confirmed by western blotting analysis and enzymatic activity assay after transfection of siRNA for 72 h.

2.12 | Cell proliferation assay

The cells were seeded into 96-well plates (PANC-1, BxPC-3, AsPC-1:2 × 10^3 cells/well; MIA Paca-2; 1 × 10^3 cells/well). At 24 h after transfection with siRNA, cell proliferation was measured using the Cell Counting Kit-8 assay (Dojindo) according to the instructions provided by the manufacturer.

2.13 | Quantitative analysis of apoptosis

Cells (5 × 10^6 cells) were transfected with siRNA and treated with gemcitabine for 72 h. Subsequently, they were washed with PBS and incubated with annexin V/fluorescein isothiocyanate and propidium iodide (PI) (Annexin V/FITC Kit; MBL International) for 15 min in the dark at room temperature according to the instructions provided by

the manufacturer. The stained cells were analyzed using an Attune NxT Flow Cytometer (Thermo Fisher Scientific).

2.14 | Mitochondrial membrane potential analysis by JC-1 staining

The mitochondrial membrane potential of PC cells was measured with the JC-1 MitoMP Detection Kit (Dojindo) according to the instructions provided by the manufacturer. Briefly, the cells transfected with siRNA for 72 h were stained with 2 μM JC-1 at 37°C for 30 min in the dark. The cells were washed with Hanks' balanced salt solution and analyzed with an Attune NxT Flow Cytometer (Thermo Fisher Scientific). Positive control cells were treated with carbonyl cyanide m-chlorophenylhydrazone (100 μM, for 90 min) prior to JC-1 staining.

2.15 | Adenovirus vector construction

We generated AdV-shGAA for the gene silencing of GAA in in vivo experiments. Two siRNA (siGAA-#1 CCAGAAAUCCUGCAGUUUA and siGAA-#3 AACCUGAGCUCCUCUGAAA) were selected from the four siRNAs against GAA (MU008881-02-0002) (GE Healthcare Dharmacon) to construct the AdV-expressing shRNA against GAA. The shRNA expression units having shGAA-1 coding siGAA-1 with the human U6 promoter and shGAA-3 coding siGAA-3 with the human U6 promoter were artificially synthesized (Eurofins Genomics, Tokyo, Japan). The AdV was constructed using the cosmid cassette pAxcwit2 containing the full-length AdV genome. The expression unit of shRNA inserted into the SnaBI cloning site located in the E4 region at 165-nt downstream from the end of the Ad5 genome.[17] The methods of preparation and purification of AdV have been previously described.[18,19] The negative control AdV-shScr has already been reported.[20] AdV were titrated using the method described by Pei et al.[21] All AdV was generated at the Core Research Facilities of Basic Science, Research Center for Medical Science (Jikei University School of Medicine). These generated protocols and experiments were approved by the Recombinant Gene Research Safety Committee of Jikei University (No. 29-58) and the Jikei University Committee for Laboratory Biosafety (No II-30-3).

2.16 | Mouse xenograft model and treatment with adenovirus vector

Mice were subcutaneously injected on one side with PANC-1 cells (5×10^6 cells per mouse). At 4 weeks after injection, mice with excessively large or small tumors were excluded. The remaining mice were randomly divided into two groups: AdV-shScr and AdV-shGAA groups. In each group, the mice received multisite intratumor injections of the corresponding recombinant virus at 1×10^9 plaque-forming units (pfu) per mouse through a single injection. Mice with tumors reaching a diameter of 20 mm and those with ulcerated tumors were killed. The tumor growth was evaluated based on the tumor size.

2.17 | Histological staining

Tumor samples were evaluated by H&E staining, anti–Ki-67, and TUNEL. Paraffin sections of tumor tissues were stained immunohistochemically using anti–Ki-67 as the primary antibody and DAKO Envision Kit/HRP as the secondary antibody (DAKO). The TUNEL assay was performed using an In Situ Cell Death Detection Kit with fluorescein (Roche Diagnostics, Basel, Switzerland) according to the instructions provided by the manufacturer. The number of Ki-67-positive cells and TUNEL-positive cells were counted in three random fields (×400 respectively) in three tumors.

2.18 | Statistical analysis

All statistical analyses were performed using the IBM SPSS statistics 25 version software (IBM). The log-rank test was performed to compare the survival. Repeated measures analysis of variance was performed to compare time-dependent tumor growth. Each in vitro sample was analyzed in triplicate. *P*-values <.05 indicated statistical significance.

3 | RESULTS

3.1 | Gemcitabine increases the levels of lysosomes and mitochondria

We performed microarray analysis of total RNA from PANC-1 cells treated with 1 μM gemcitabine to identify the key responsive gene involved in chemoresistance to this agent. Although decreased expression of approximately 70 genes was observed in gemcitabine-treated PANC-1 cells compared with control, the expression of approximately 100 genes was significantly upregulated (Figure 1A). Among the responsive genes, some lysosomal genes (LAMP2 and LAMP3), an autophagy-related gene (microtubule-associated protein 1 light chain 3 beta [MAP1LC3B]), and a mitochondrial gene (mitofusin 2 [MFN2]) were upregulated (Figure 1B). We analyzed the PANC-1 and MIA PaCa-2 cells following 48 h of incubation with gemcitabine (PANC-1:1 μM; MIA PaCa-2:.5 μM) by electron microscopy to confirm the effect of gemcitabine on those organelles in PC cells. TEM analysis revealed the presence of electron-dense lysosomes and slightly swelled mitochondria in gemcitabine-treated PC cells (Figure 1C). Enhanced fluorescence intensities of LysoTracker (red) and MitoTracker (green) were also observed in PANC-1 and MIA PaCa-2 cells treated with gemcitabine (Figure 1D). Indeed, flow cytometric analysis showed that the mean fluorescence intensity of MitoTracker was significantly increased in gemcitabine-treated PC

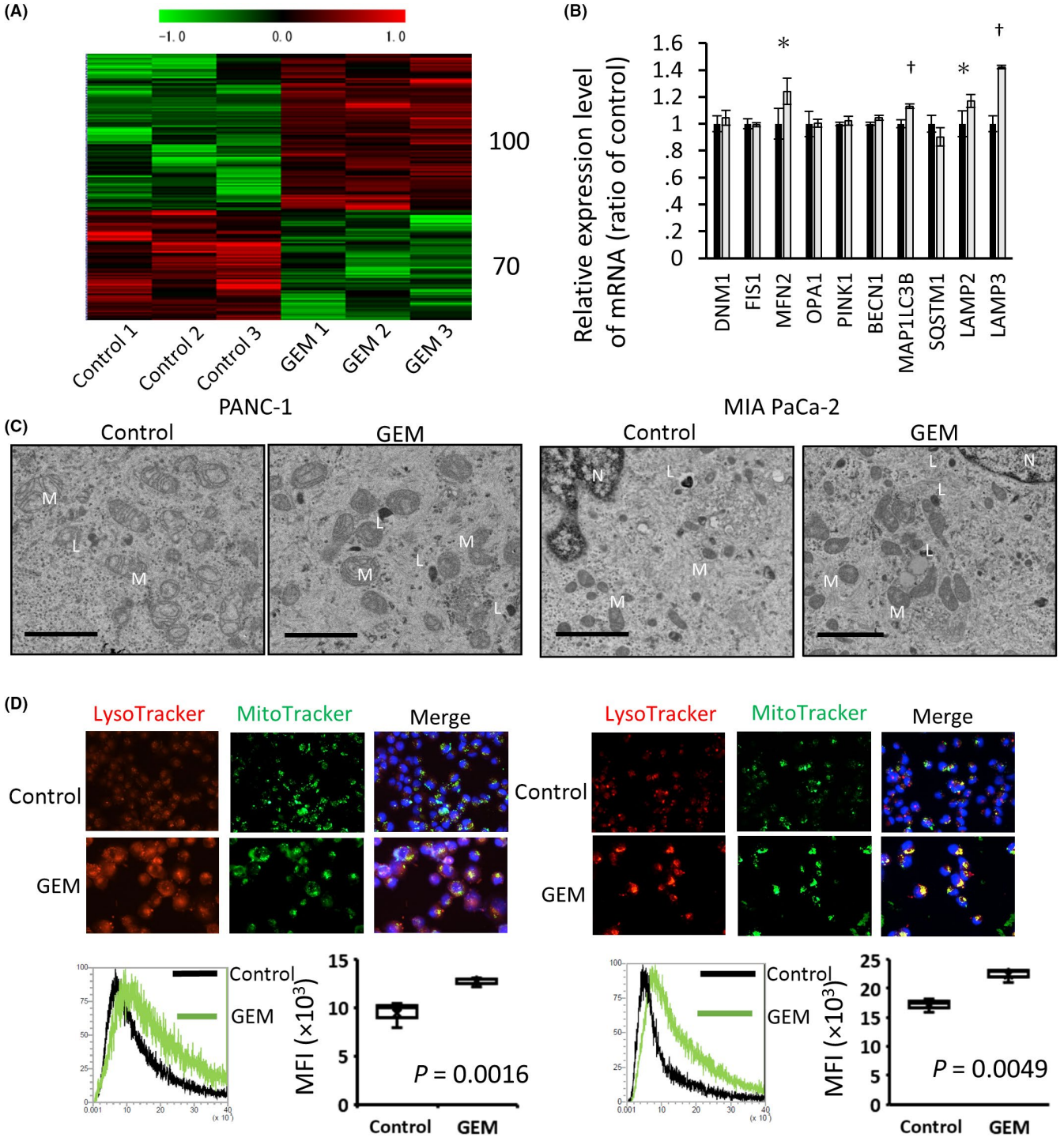

FIGURE 1 Gemcitabine increases levels of the lysosomes and mitochondria in pancreatic cancer cells. (A,B) RNA-Seq data analysis of PANC-1 cells after treatment with or without GEM 24 h. (A) A total of 100 genes were significantly upregulated in response to treatment with GEM. (B) Autophagy–lysosome associated genes were upregulated. (C) TEM images revealed ultrastructure of PANC-1 and MIA PaCa-2 cells treated with or without GEM (PANC-1; 1 μM, MIA PaCa-2; 0.5 μM) for 48 h. L, lysosome; M, mitochondria; N, nucleus. Scale bar: 2 μm. (D) Fluorescent microscopy images of PANC-1 and MIA PaCa-2 cells treated with or without GEM (PANC-1; 1 μM, MIA PaCa-2; 0.5 μM) for 48 h. Cells were stained with LysoTracker (red) and MitoTracker (green). Nuclei were counterstained with DAPI (blue). Quantification of the expression of mitochondria with or without GEM treatment by FCM

cells compared with non–treated cells (Figure 1D). These results indicated that chemoresistance-inducible sublethal concentration of gemcitabine increases the amounts of lysosomes and mitochondria in PC cells.

3.2 | Gemcitabine enhances acid alpha-glucosidase expression and enzymatic activity

We analyzed the 52 typical lysosomal genes in the RNA microarray data of gemcitabine-treated PANC-1 cells to investigate whether lysosomal function is involved in chemoresistance to this agent. The relative mRNA expression levels of 33 of 52 genes increased in PANC-1 cells 24 h after treatment with gemcitabine (Figure 2A). In particular, glycosidases, such as GAA and α-galactosidase A, were included in the top five genes of the upregulated 33 genes. In this study, we focused on the GAA, which is a key enzyme for glycogen metabolism. Furthermore, basic GAA enzyme activity and basic expression levels of autophagy-related proteins, such as LC3 and SQSTM1/p62, were found to differ between cell lines (Figure S1A and B). We analyzed the enzymatic activity of GAA in the gemcitabine-treated PC cells, including PANC-1 and MIA PaCa-2 cells, to confirm the effect of the treatment on GAA. The enzymatic activity of GAA was significantly enhanced in PC cells after treatment with gemcitabine in a dose–dependent and time–dependent manner (Figure 2B and D Figure S1C and D). Corresponding to the enzymatic activity, increased levels of GAA proteins were also observed in gemcitabine-treated PC cells (Figure 2D,E; Figure S1E). These results indicated that treatment with gemcitabine increases the expression of GAA in PC cells. In addition, western blotting analysis revealed that increased levels of LC3-II and decreased levels of SQSTM1/p62 were observed in PC cells. This finding suggested that gemcitabine-enhanced lysosomal function promotes autophagic flux in PC cells (Figure 2C,E; Figure S1E).

3.3 | Knockdown of acid alpha-glucosidase improves the antitumor effect of gemcitabine

We analyzed the cell proliferation and induction of apoptosis in gemcitabine-treated PANC-1 and MiaPaCa-2 cells transfected with siRNA against GAA gene (siGAA) to evaluate the effect of GAA modulation on the sensitivity of PC cells to gemcitabine. Although cell viability in both control and GAA-knockdown cells was suppressed by treatment with gemcitabine in a dose–dependent manner (Figure 3A; Figure S2A), GAA-knockdown cells showed higher sensitivity to a low dose of gemcitabine (range: 0-1 μM) than control cells. In addition, the combination of GAA knockdown and treatment with gemcitabine suppressed the proliferation rate of PC cells compared to treatment with gemcitabine alone (Figure 3B; Figure S2B). Subsequently, we performed western blotting analysis of cleaved CASP8, CASP3, and cleaved PARP to investigate whether GAA knockdown affects apoptotic signals in PC cells. Suppression of GAA expression increased the levels of these apoptotic signals in PC cells 72 h after treatment with sublethal concentrations of gemcitabine (PANC-1:1 μM; MIA PaCa2: 0.5 μM) (Figure 3C; Figure S2C and D). Moreover, the annexin V assay revealed that knockdown of GAA increased the number of apoptotic cells in PC cells 72 h after treatment with gemcitabine (Figure 3D; Figure S2E), indicating that induction of the apoptotic cascade is one of the main inhibitory effects of GAA modulation on the proliferation of PC cells. Altogether, knockdown of GAA improved the sensitivity of PC cells to sublethal concentrations of gemcitabine.

We also found that knockdown of GAA decreased cell viability in gemcitabine-treated PC cells and untreated cells (Figure 3A,B). Following the suppression of GAA expression in PC cells, we observed a time-dependent inhibitory effect of GAA knockdown on cell proliferation, corresponding to a reduction in the enzymatic activity and protein levels of GAA (Figure S3A–C). Because antiproliferative effects were observed when several types of siRNA were used (Figure S3D), these effects did not seem to be off–target effects. In addition, knockdown of GAA increased the levels of cleaved PARP and several caspases, and both ratios of early and late apoptosis in PC cells (annexin V+/PI− and annexin V+/PI+) (Figure 3C,D). These results suggested that GAA is a promising target for improving chemosensitivity and developing novel therapies against PC cells.

3.4 | Suppression of acid alpha-glucosidase accumulates depolarized mitochondria

Using TEM, we analyzed the morphological changes of intracellular organelles in PANC-1 and MiaPaCa-2 cells transfected with siGAA to further investigate the effect of GAA knockdown on PC cells. Although there was no obvious accumulation of autophagosomes observed, the levels of enlarged lysosomes and abnormal morphological mitochondria were increased in PANC-1 cells (Figure 4A). Lysosomal and mitochondrial changes in GAA-knockdown MiaPaCa-2 cells were relatively less pronounced than those noted in GAA-knockdown PANC-1 cells (Figure 4A; Figure S4A), corresponding to the levels of GAA proteins and their activity (Figure S1A,B). Following the staining of GAA-knockdown PC cells with pH-responsive Dye LysoTracker, we observed decreased fluorescence intensity (Figure 4B; Figure S4B), suggesting that GAA knockdown affects the pH level of lysosomes in PC cells.

FIGURE 2 Gemcitabine enhances acid alpha-glucosidase (GAA) expression and enzymatic activity. (A) Relative expression levels of lysosomal enzyme with treatment of GEM. Thirty-three lysosomal enzyme genes were upregulated with GEM treatment. (B) Pancreatic cancer (PC) cells were treated with 0-20 μM GEM for 48 h. GAA enzyme activities were enhanced in a dose–dependent manner in both cells. (C) The expression levels of GAA, LC3, and p62 were assessed by western blotting after 72 h of GEM treatment. (D) Enzyme activities of GAA were measured with GEM (PANC-1, 1 μM; MIA PaCa-2, 0.5 μM) for 24, 48, and 72 h. (E) The expression levels of GAA, LC3, and p62 were assessed by western blotting after 24, 48, and 72 h of GEM treatment. Data were mean values of three independent experiments. Values are expressed as the mean ± SD (*$P < .05$; †$P < .01$, vs untreated)

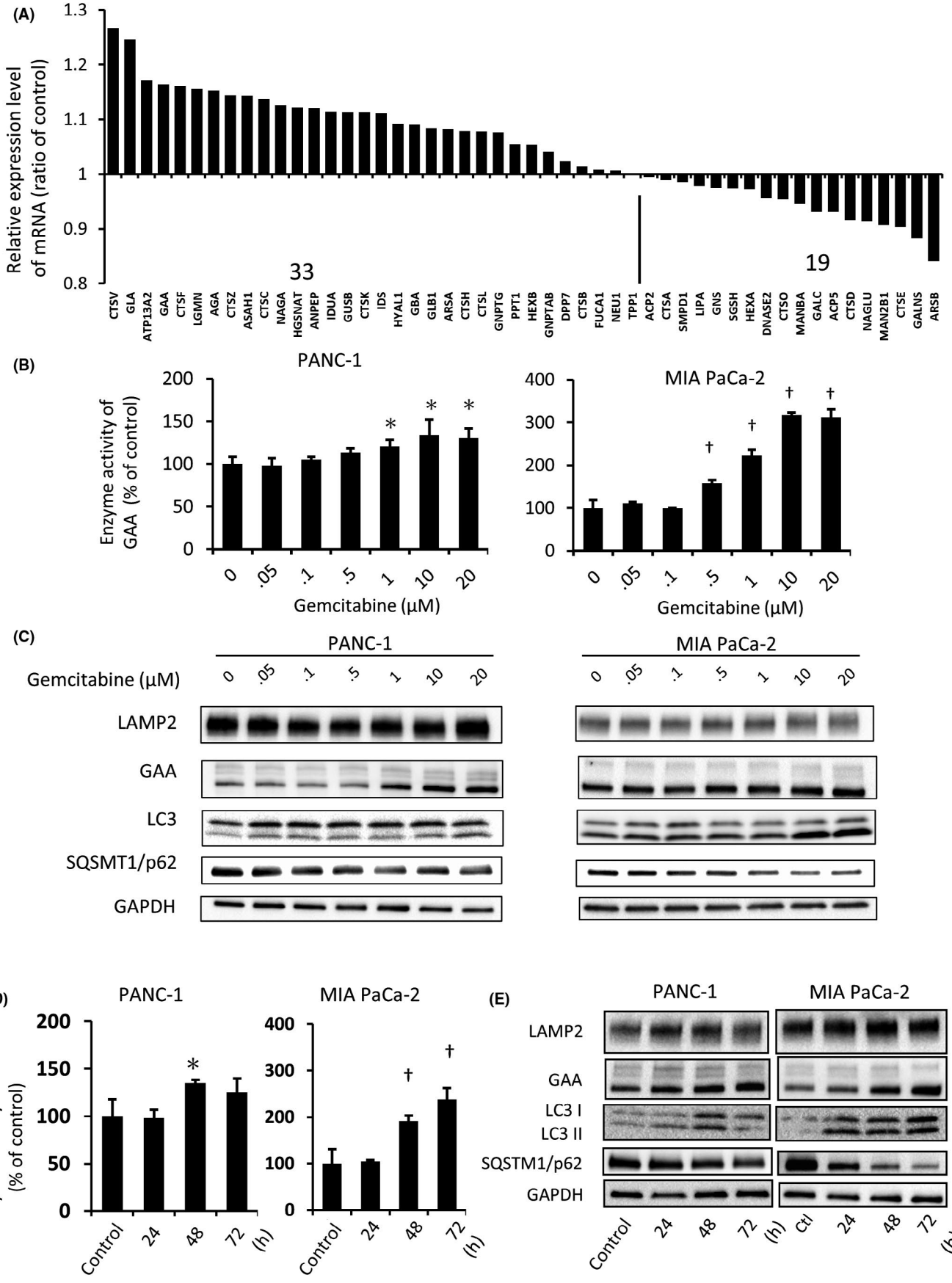
(A)
Relative expression level of mRNA (ratio of control)
1.3
1.2
1.1
1
0.9
0.8
33
19
CTSV GLA ATP13A2 GAA CTSF LGMN AGA CTSZ ASAH1 CTSC NAGA HGSNAT ANPEP IDUA GUSB CTSK IDS HYAL1 GBA GLB1 ARSA CTSH CTSL GNPTG PPT1 HEXB GNPTAB DPP7 CTSB FUCA1 NEU1 TPP1 ACP2 CTSA SMPD1 LIPA GNS SGSH HEXA DNASE2 CTSO MANBA GALC ACP5 CTSD NAGLU MAN2B1 CTSE GALNS ARSB
(B)
PANC-1
MIA PaCa-2
Enzyme activity of GAA (% of control)
Gemcitabine (μM)
0 .05 .1 .5 1 10 20
(C)
PANC-1
MIA PaCa-2
Gemcitabine (μM)
LAMP2
GAA
LC3
SQSMT1/p62
GAPDH
(D)
PANC-1
MIA PaCa-2
Enzyme activity of GAA (% of control)
Control 24 48 72 (h)
(E)
PANC-1
MIA PaCa-2
LAMP2
GAA
LC3 I
LC3 II
SQSTM1/p62
GAPDH
Control 24 48 72 (h) Ctl 24 48 72 (h)

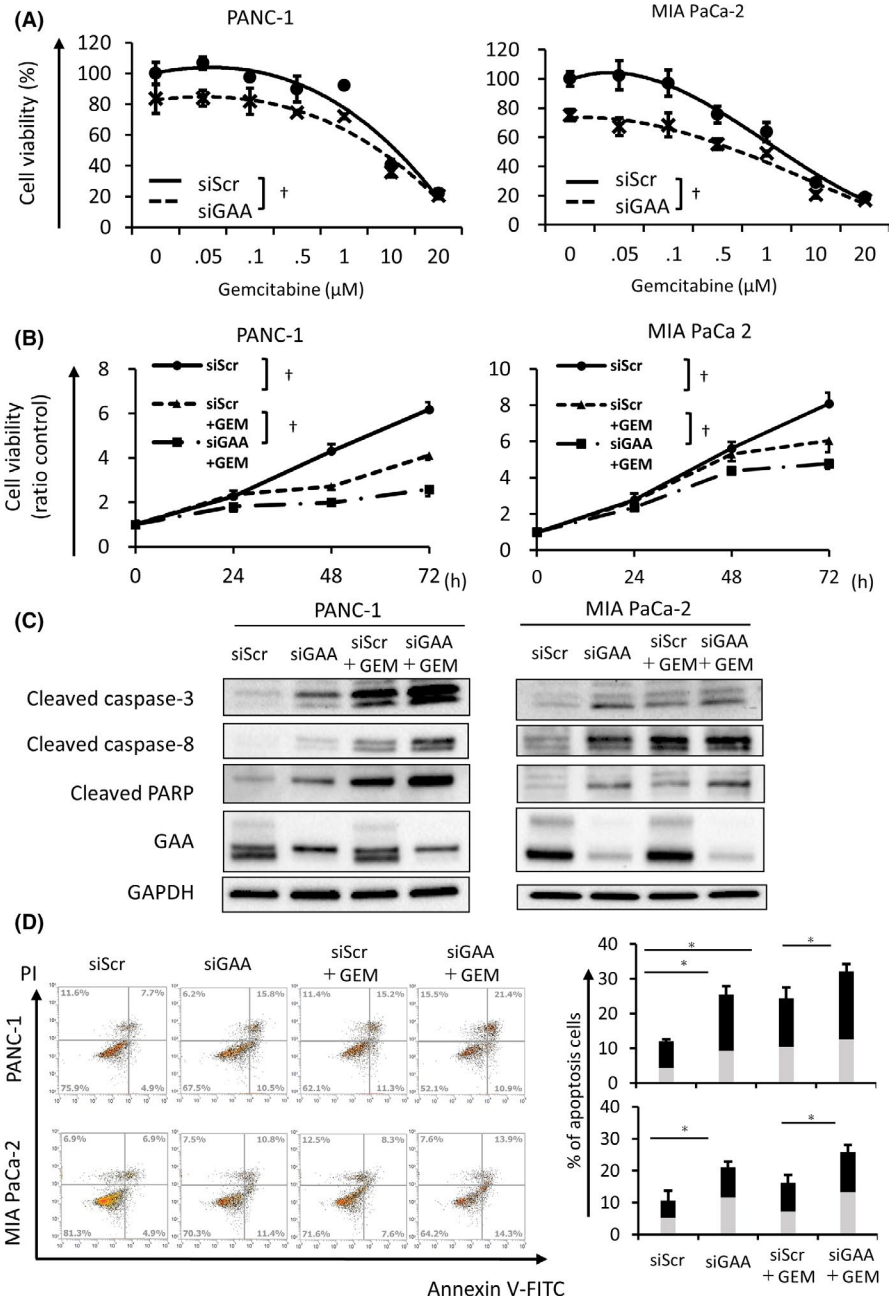

FIGURE 3 Knockdown of acid alpha-glucosidase (GAA) improves the antitumor effect of GEM. (A) Pancreatic cancer cell lines were transfected with siRNA and treated with a range of GEM concentrations (PANC-1, MIA PaCa-2; GEM, 0-20 μM) for 72 h. The cell proliferation of each cell was suppressed by GEM in a dose–dependent manner. (B) Cell viabilities of PANC-1 and MIA PaCa-2 at 24, 48, and 72 h after treatment with GEM (PANC-1; 1μM, MIA PaCa-2; 0.5 μM) were shown as the fold change. In the cell proliferation assay, KD of GAA enhanced the anti–proliferation effects of GEM in PANC-1 and MIA PaCa-2 cells. (C) Western blot analysis demonstrated the expression levels of apoptosis-related proteins. The levels of cleaved caspase-3 and −8 as well as cleaved PARP were greater than those in GEM alone. (D) The quantification of apoptotic cells was analyzed by annexin V/PI assay at 72 hours after GEM treatment. The number of apoptotic cells in combination of GAA KD and GEM were greater than those in GEM alone group. Data are presented as the mean ± SD from three independent experiments (*$P < .05$)

In contrast, MitoTracker staining revealed the significantly increased mean fluorescence intensity in GAA-knockdown cells versus control cells (Figure 4B,C), indicating that GAA knockdown accumulates mitochondria in PC cells. We analyzed the membrane potential of mitochondria in GAA-knockdown PC cells using the fluorescent dye JC-1 to evaluate the mitochondrial function. This dye is capable of selectively entering into mitochondria and changing from a red to green signal with depolarization of the mitochondrial membrane potential. Fluorescence microscopic and flow cytometric analyses showed that the level of green signal was significantly increased in PC cells treated with siGAA and the depolarization inducer carbonyl cyanide m-chlorophenylhydrazone (Figure 4D,E), indicating that accumulated mitochondria in PC cells treated with siGAA are depolarized. These results suggested that GAA knockdown accumulates dysfunctional mitochondria in PC cells.

3.5 | Suppression of acid alpha-glucosidase inhibited autophagy flux by regulation of transcription factor EB

Accumulated dysfunctional mitochondria are generally degraded by mitophagy, a process termed mitochondrial selective autophagy.[22,23] We compared the expression levels of autophagy-related protein with bafilomycin A1 (an autophagy inhibitor)-treated PC cells to investigate whether GAA knockdown accumulates mitochondria due to blocked autophagy or suppressed autophagy flux. Bafilomycin A1 has been previously used in the analysis of autophagy as an inhibitor of fusion between autophagosomes and lysosomes. As expected, the accumulation of LC3II and SQSTM1/p62 was observed in bafilomycin A1-treated PC cells (Figure 5A,B and Figure S5A). In contrast,

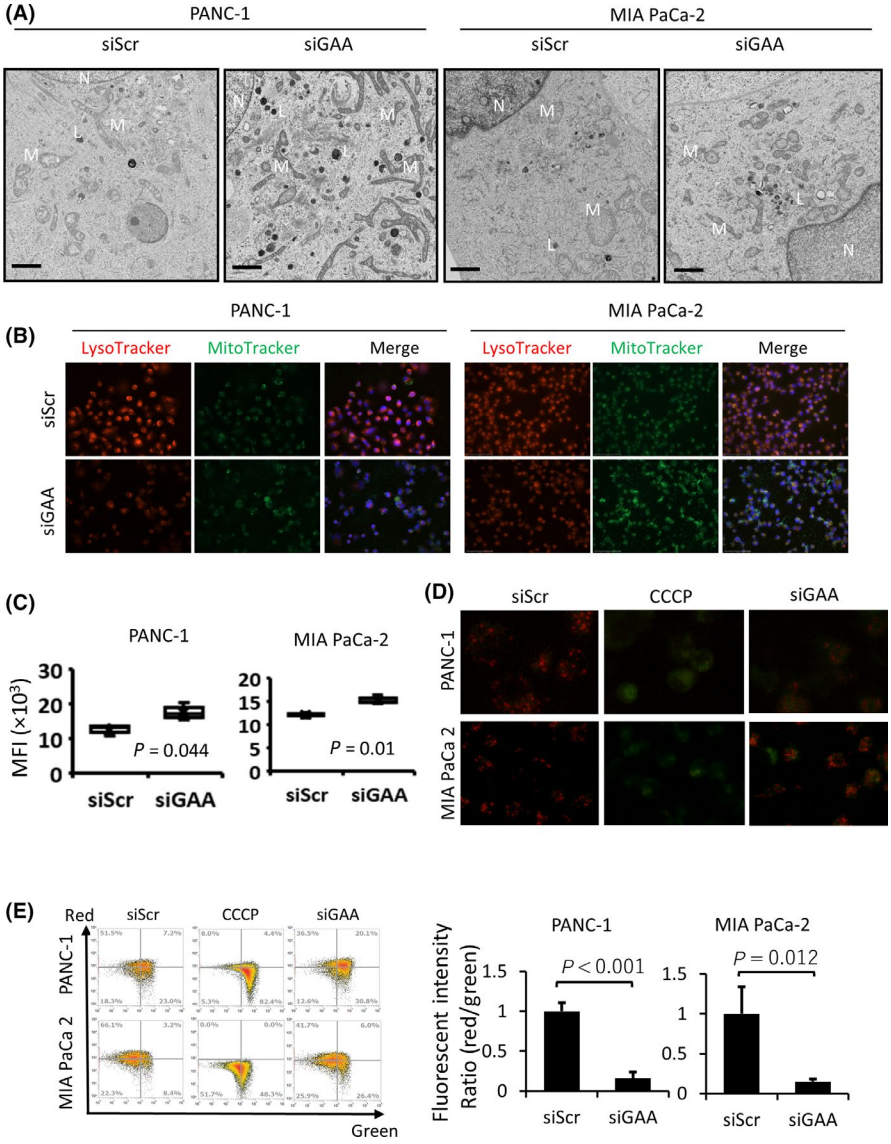

FIGURE 4 Suppression of acid alpha-glucosidase (GAA) accumulates the depolarized mitochondria. (A) The effects of siGAA transfection for intracellar organelles were observed with TEM for 72 h after siRNA transfection. Mitochondrial changes were particularly prominent in PANC-1 cells. L, lysosome; M, mitochondria; N, nucleus. Scale bar: 2 μm. (B) Fluorescence microscopy of LysoTracker red was reduced in PANC-1 and MIA PaCa-2 cells with KD of GAA. Scale bar: 100 μm. (C) FCM showed the increase of mitochondria in pancreatic cancer (PC) cells (PANC-1, $P = .044$, MIA PaCa-2, $P = .01$). (D) Cells were stained with JC1 probe, and immunostaining showed the red to green change of JC1 with siGAA. (E) FCM showed the downregulation of the red/green fluorescence ratio (PANC-1, $P < .001$; MIA PaCa-2, $P = .012$, retrospectively)

despite the accumulation of mitochondria, accumulation of LC3II and SQSTM1/p62 was not observed in GAA-knockdown cells. In addition, the expression level of LAMP2, a membrane protein of lysosome, was increased in GAA-knockdown cells. Knockdown of GAA affects the pH of the lysosome and inactivates the accumulation of LAMP2 but not that of LC3II and SQSTM1/p62; this suggested that impaired lysosomes could fuse with the autophagosome, but the ability for degradation was decreased.

Furthermore, the nuclear translocation of TFEB in GAA-knockdown PC cells was evaluated to determine the initiation of autophagy in these cells. In PANC-1 cells, the nuclear translocation of TFEB was decreased and the cytoplasmic levels of TFEB were suppressed (Figure 5C; Figure S5B). Furthermore, the translocation of TFEB was activated within 24 h and its total expression was deescalated in a time-dependent manner (Figure S5C). Considering the poor effect of autophagy inhibition and suppression of TFEB regulation, knockdown of GAA accumulated the malfunctioning mitochondria and inhibited the autophagy flux.

3.6 | Adenovirus vector with shGAA exerts an oncolytic effect on pancreatic cancer tumors *in vivo*

We generated an Adv-shGAA vector to investigate the oncolytic effects of GAA knockdown in vivo. From the four siRNAs against GAA, those with the highest efficiency for the suppression of GAA expression were selected (Figure S3D) and the AdV for shGAA was constructed (Figure S5D). The effect of AdV was confirmed by western blotting analysis (Figure S5E) in vitro. This was followed by direct injection (1×10^9 pfu) into the tumors formed by subcutaneous transplantation of PANC-1 cells in nude mice. At 4 weeks after injection, the tumor size in the Adv-shGAA group was significantly smaller than that recorded in the Adv-shScr group (Figure 6A). Although there was no significant difference in body weight between the Adv-shGAA and Adv-shScr groups, prolonged survival rates were noted in the former group (Figure 6B,E). Adv-shGAA decreased GAA enzymatic activity and proteins and increased the levels of cleaved CASP3 in PC tumors (Figure 6C,D). Histological

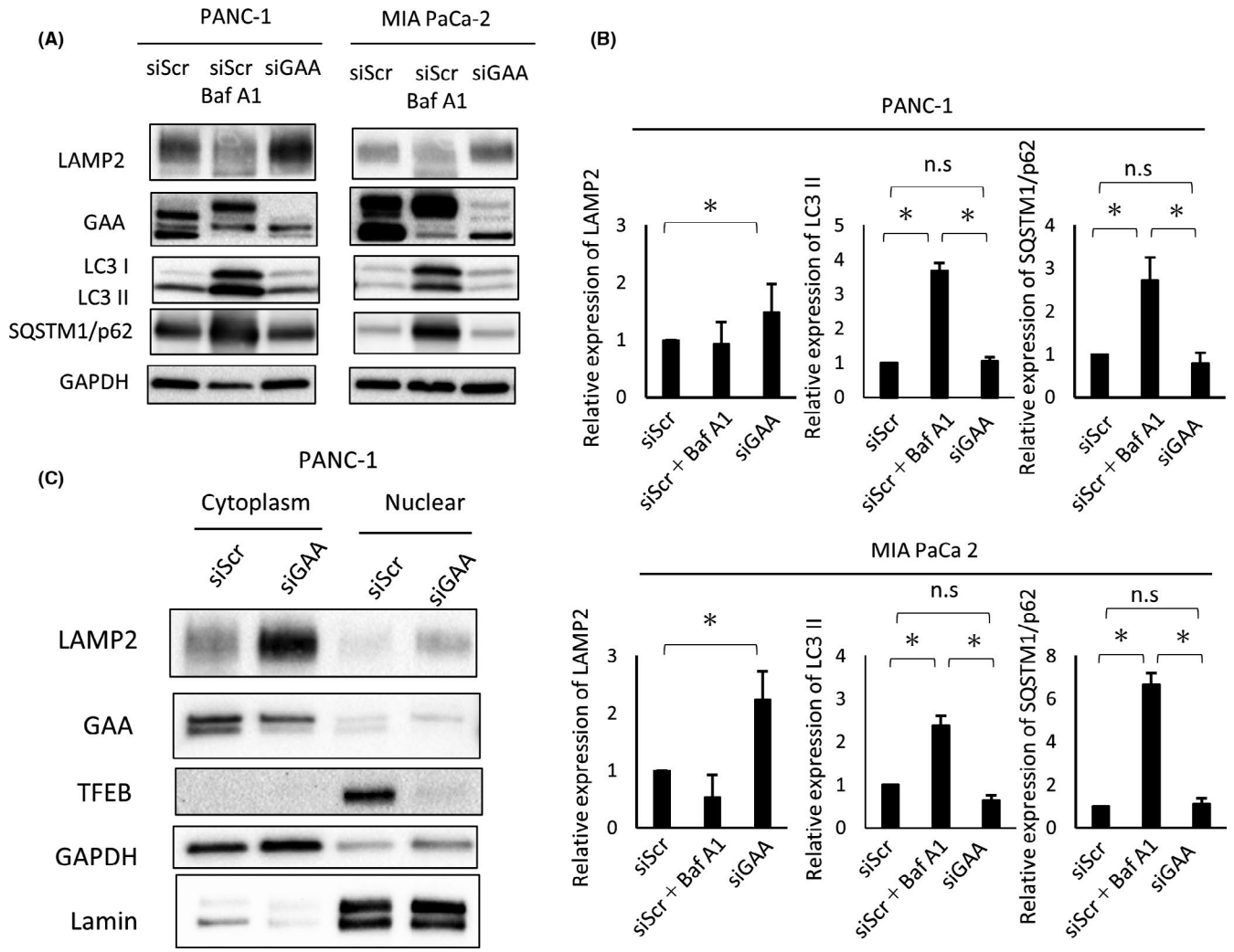

FIGURE 5 Suppression of acid alpha-glucosidase (GAA) inhibited transcription factor EB (TFEB) nuclear migration and suppressed autophagy flux. (A) Western blot analysis demonstrated the expression of autophagy-related proteins. The expression levels of LC3 I and II were not upregulated in siGAA cells compared with Bafilomycin A1 (100 nM). (B) The expression levels of LAMP2 were increased in siGAA cells, and those of LC3 II and SQSTM1/p62 were less than those in the Bafilomycin A1 group, respectively ($P < .05$ each). (C) Western blot analysis demonstrated that the suppression of TFEB nuclear migration and LAMP2 expression was accumulated in GAA KD cell. Data are presented as the mean ± SD from three independent experiments (*$P < .05$)

analysis revealed decreased numbers of Ki67-positive cells and increased numbers of TUNEL-positive cells in Adv-shGAA-injected tumors (Figure 6F). Furthermore, obvious accumulation of mitochondria in the tumors derived from the Adv-shGAA group, similar to that observed in PANC-1 cells in vitro (Figure 6G). These results indicated that Adv-shGAA is a promising vector for oncolytic gene therapy against PC.

4 | DISCUSSION

In this study, through microscopic analysis and molecular biological analysis (including RNA microarray and western blotting), we found that treatment with gemcitabine increases the lysosomes in PC cells (Figures 1 and 2). We also demonstrated that the lysosomal enzyme GAA is a one of the genes responsive to treatment with gemcitabine

FIGURE 6 Adenovirus vector with shGAA has an oncolytic effect on pancreatic cancer (PC) tumors in vivo. (A) Tumor growth curves were plotted. The tumor growth was suppressed ($P = .04$) in the Adv-shGAA group. (B) Kaplan-Meyer curve of mice after AdV injection. Tumor-rerated survival was prolonged ($P = .034$) in the Adv-shGAA group. Median tumor diameter and tumor-related survival were recorded twice a week. (C) GAA enzyme activity was suppressed in the Adv-shGAA group. (D) The expression of GAA protein was suppressed, and cleaved caspase-3 was overexpressed in the Adv-shGAA group. (E) Body weight change during the experiment. There was no difference between Adv-shScr and Adv-shGAA groups. (F) Enucleated tumors were stained with H&E and anti–Ki-67. The ratio of Ki-67 positive cells (arrowheads) was reduced in the tumor of the Adv-shGAA group. (G) TEM observed the defective mitochondria in the tumor of the Adv-shGAA group. L, lysosome; M, mitochondria; N, nucleus. Scale bar: 50 nm

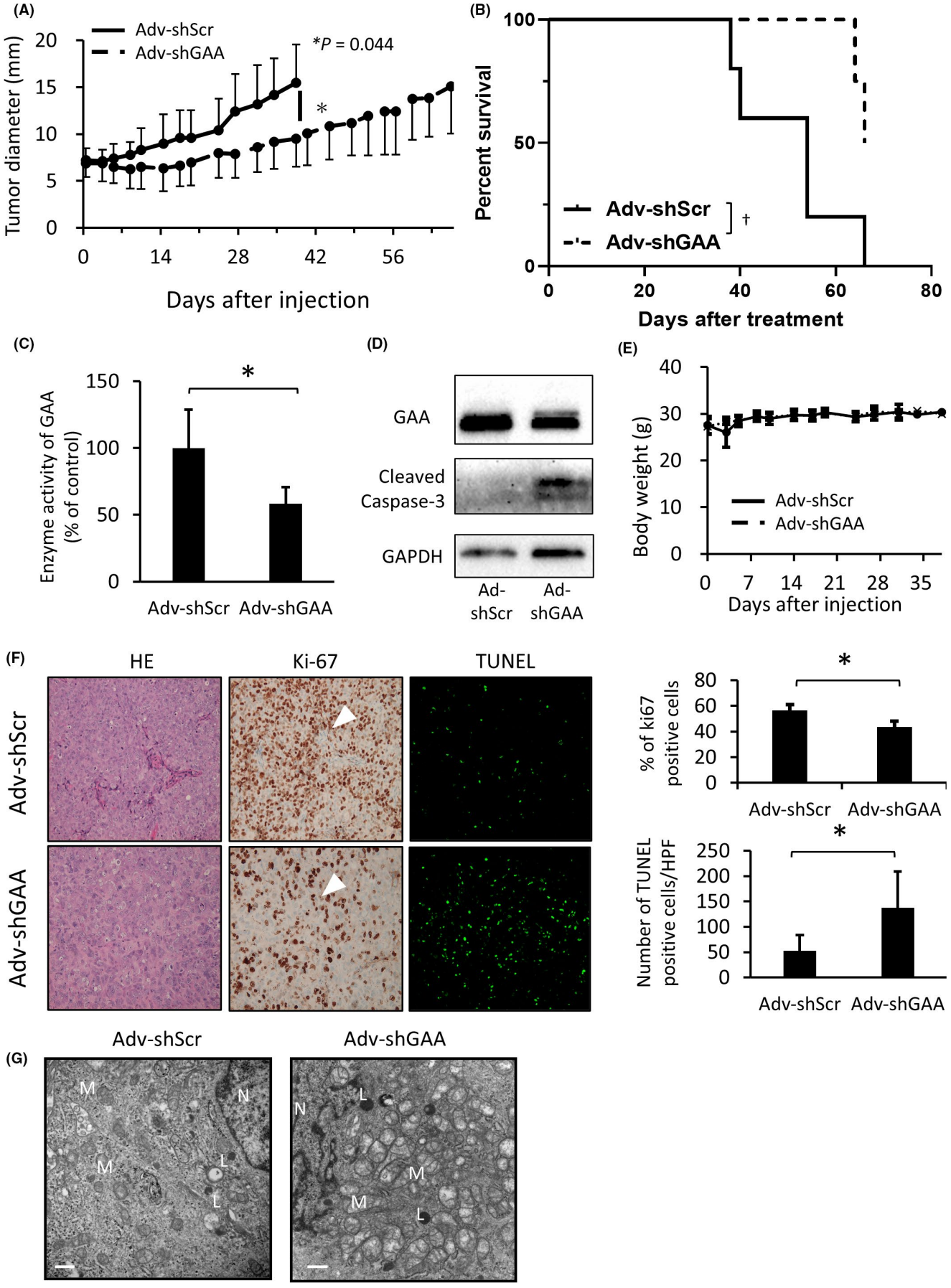
(A)
Adv-shScr
Adv-shGAA
*P = 0.044
Tumor diameter (mm)
Days after injection
(B)
Percent survival
Adv-shScr
Adv-shGAA
†
Days after treatment
(C)
Enzyme activity of GAA (% of control)
Adv-shScr
Adv-shGAA
(D)
GAA
Cleaved Caspase-3
GAPDH
Ad-shScr
Ad-shGAA
(E)
Body weight (g)
Adv-shScr
Adv-shGAA
Days after injection
(F)
HE
Ki-67
TUNEL
Adv-shScr
Adv-shGAA
% of ki67 positive cells
Number of TUNEL positive cells/HPF
(G)
Adv-shScr
Adv-shGAA
M
N
L

in PC cells (Figures 1 and 2). Autophagy has attracted attention as a factor of poor prognosis and as a therapeutic target for some cancer cells.[24] In PC cells, upregulation of TFEB is required for tumor extension. Because complete inhibition of autophagy suppresses tumor progression in several carcinomas,[25-29] studies have been attempting to regulate autophagy using several small molecules, such as chloroquine and bafilomycin A1.[30-32] In addition, several clinical trials have demonstrated the efficacy of treatment with autophagy inhibitor alone or a combination of chemotherapeutic agents through the improvement of chemosensitivity.[33] In contrast, although autophagy involves autophagosomes and lysosomes, lysosomal regulation has received minimal attention as a therapeutic target for cancer. Our results demonstrated that suppression of GAA improves the sensitivity to gemcitabine in PC cells and induces apoptosis in tumors by modulation of TFEB translocation (Figures 3-5). These findings indicated that GAA is a promising target for the development of novel therapies against PC. To the best of our knowledge, the present study is the first to report that suppression of mono–lysosomal enzyme exerts an anticancer effect on PC cells.

Lysosomal degradation plays a crucial role in biological macromolecule metabolism, cell growth, cell division, and cell differentiation in cancer and normal cells[34] For example, the enhanced lysosomal degradation is observed in several types of cancer cells, and is involved in angiogenesis and their ability to metastasize.[35] However, the role of lysosomal degradation in response to chemotherapy has not been fully elucidated. In our study, we found that increased levels of lysosomes are observed in PC cells after treatment with gemcitabine (Figure 2). In addition, gemcitabine increased the relative mRNA expression levels of 33 of 52 genes in PC cells (Figure 2A). Among the 33 upregulated genes, the top five genes consisted of glycosidases (GAA and α-galactosidase A), proteases (cathepsin V and cathepsin F), and an ATPase (ATP13A2) (Figure 2A). Western blotting analysis detected increased levels of LC3-II and decreased levels of p62 in gemcitabine-treated PC cells. However, TEM analysis did not show obvious accumulation of typical autophagosomes in these cells, despite increased levels of lysosomes (Figures 1 and 2). In addition, the enzymatic activity of GAA is increased by gemcitabine. GAA is the most efficient lysosomal enzyme for glycolysis as it breaks down glucose bonds. Cancer cell metabolism is dependent on a phenomenon known as the Warburg effect, which favors a high rate of glycolysis followed by lactate fermentation. The cytotoxic effects of gemcitabine activate the glycolytic system, which is believed to enhance the activity of GAA. These findings suggested that enhanced lysosomal degradation promotes autophagic flux in gemcitabine-treated PC cells. Therefore, it appears that lysosomal degradation abilities, which originate from glycosidases and proteases, are involved in the key resistance mechanism to cytotoxicity in PC cells after treatment with gemcitabine. This notion is supported by previous evidence stating that chloroquine, a global lysosomal enzyme inhibitor increasing the pH in lysosomes, enhances gemcitabine-induced apoptosis through the production of ROS in PC cells.[30-32]

Suppression of lysosomal activity is a promising therapeutic approach for PC. However, complete inhibition of lysosomal degradation affects various intracellular phenomena, including cytoprotective autophagy, in normal cells. Indeed, although treatment with chloroquine exerted a tumor-suppressive effect in a rat model of chemically-induced hepatocarcinoma, the agent accelerates hepatocarcinogenesis in the dysplastic stage.[36] Therefore, selective and regulatable inhibition of lysosomal function is key for the discovery of novel therapies against cancer. In this study, we showed the therapeutic effectiveness of GAA modulation in PC cells using siGAA and AdV-shGAA (Figures 3-6). GAA is one of the lysosomal hydrolases and catalyzes the degradation of intracellular glycogen to glucose in lysosomes. Genetic deficiency of GAA results in glycogen storage disease type II, which is characterized by massive deposits of glycogen accompanied by autophagosomal accumulation.[37] Mitochondrial accumulation is also observed in skeletal muscle from GAA-deficient mice or humans with multiple mitochondrial defects, such as a decrease in membrane potential and an increase in ROS.[37] We found that suppression of GAA accumulated malfunctioning mitochondria in PC cells (Figure 4). In addition, residual GAA activity was observed in GAA-knockdown PC cells (Figure S4E), suggesting that those cells mimic a milder phenotype of glycogen storage disease type II.

Our result showed that knockdown of GAA decreases cell proliferation and increases the apoptotic signals in PC cells accompanied by accumulation of dysfunctional mitochondria (Figure 5). Furthermore, we found that mitochondrial accumulation in GAA-knockdown PC cells is caused by the suppression of TFEB. Because the basal metabolism by autophagy is enhanced in PC due to increased TFEB, inhibition of TFEB expression regulates autophagy flux and causes the accumulation of intracellular organelles, including mitochondria. As a key mediator of chemoresistance and apoptosis, mitochondria have been identified as signaling molecules in various intracellular pathways that regulate both cell survival and cell death.[12,38] In particular, because mitochondria release ROS and cytochrome C, accumulated dysfunctional mitochondria can contribute to the induction of cell apoptosis. We found that treatment with gemcitabine or siGAA alone increases the amounts of mitochondria in PC cells (Figures 1C and 5C). Combination treatment with gemcitabine and siGAA also increases the levels of apoptotic-signaling proteins in PC cells versus those recorded in cells treated with gemcitabine or siGAA alone (Figure 4A). There could be two reasons for this improvement in the antitumor effect of gemcitabine following the knockdown of GAA: (a) dysfunctional lysosomes impaired the degeneration in autophagosomes, resulting in the accumulation of defective mitochondria; and (b) lysosomal dysfunction suppressed the master regulator TFEB and suppressed the autophagy flux. Therefore, the accumulation of mitochondria and regulation of TFEB is one of the key factors for the anticancer effects induced by GAA knockdown.

In this study, we demonstrated the promising effect of treatment with Adv-shGAA on tumors using a xenograft mouse model (Figure 6). Gene therapy has attracted interest as an emerging treatment option for cancer in the clinical setting.[39-42] For example, tumor-specific oncolytic viral vectors, such as talimogene laherparepvec, are approved by the United States Food and Drug Administration and

the European Medicines Agency. AdV are frequently used vectors in oncolytic viruses.[43-45] AdV do not integrate their genes into the host genome, and some of them avoid the host immune response and suppress liver damage.[42] Because integration of the viral gene into the genome of host cells is not caused by transfection of AdV, this vector may be safe and suitable for gene therapy in the treatment of cancer.[39] Importantly, a single administration of Adv-shGAA, which consists of human U6 promoter-driven shGAA, exhibited antitumor effects without inducing obvious side effects. Therefore, downregulation of GAA by AdV may be a promising oncolytic gene therapy.

In summary, enhancement of lysosomal activity was involved in resistance to treatment with gemcitabine in PC cells. Knockdown of the GAA gene disturbs the quality control of damaged mitochondria in PC cells through impairment of lysosomal function. Moreover, knockdown of GAA enhances the antitumor effect of treatment with gemcitabine in PC cells. Gene therapy with AdV-shGAA may be a new strategy for the treatment of PC.

ACKNOWLEDGMENTS

Toshiaki Tachibana and Emi Kikuchi (Core Research Facilities of Basic Science, Research Center for Medical Science, Jikei University School of Medicine), cooperate in transmission electric microscopy. Takashi Higuchi (Division of Gene Therapy, Research Center for Medical Science, Jikei University School of Medicine) provided advice on experimental techniques. This work was supported by the Japan Society for the Promotion of Science (JSPS) KAKENHI Grant Number 17K16584 and 20K17665 (Dr Yoshihiro Shirai), the Uehara Memorial Foundation Research Incentive Grant and the Jikei University Research Fund.

DISCLOSURE STATEMENT

The authors declare no potential conflicts of interest.

DATA AVAILABILITY STATEMENT

The data of generated AdV can be referenced from corresponding author upon request. The microarray analysis data are deposited into Gene Expression Omnibus with the accession code GSE153460. All other data are available from the corresponding author upon request.

ORCID

Ryoga Hamura https://orcid.org/0000-0003-1670-4435
Yoshihiro Shirai https://orcid.org/0000-0002-4907-0101
Naoki Takada https://orcid.org/0000-0003-3192-7979

REFERENCES

1. Levine B, Kroemer G. Autophagy in the pathogenesis of disease. *Cell*. 2008;132:27-42.
2. Guo JY, Xia B, White E. Autophagy-mediated tumor promotion. *Cell*. 2013;155:1216-1219.
3. Kimmelman AC. The dynamic nature of autophagy in cancer. *Genes Dev*. 2011;25:1999-2010.
4. Perera RM, Stoykova S, Nicolay BN, et al. Transcriptional control of autophagy-lysosome function drives pancreatic cancer metabolism. *Nature*. 2015;524:361-365.
5. Yang S, Wang X, Contino G, et al. Pancreatic cancers require autophagy for tumor growth. *Genes Dev*. 2011;25:717-729.
6. Guo JY, Chen HY, Mathew R, et al. Activated Ras requires autophagy to maintain oxidative metabolism and tumorigenesis. *Genes Dev*. 2011;25:460-470.
7. Perera RM, Bardeesy N. Pancreatic cancer metabolism: breaking it down to build it back up. *Cancer Discov*. 2015;5:1247-1261.
8. Rubinsztein DC, Codogno P, Levine B. Autophagy modulation as a potential therapeutic target for diverse diseases. *Nat Rev Drug Discovery*. 2012;11:709-730.
9. Schröder BA, Wrocklage C, Hasilik A, Saftig P. The proteome of lysosomes. *Proteomics*. 2010;10:4053-4076.
10. Shimada Y, Klionsky DJ. Autophagy contributes to lysosomal storage disorders. *Autophagy*. 2012;8:715-716.
11. Pattingre S, Tassa A, Qu X, et al. Bcl-2 antiapoptotic proteins inhibit Beclin 1-dependent autophagy. *Cell*. 2005;122:927-939.
12. Bernardini JP, Lazarou M, Dewson G. Parkin and mitophagy in cancer. *Oncogene*. 2017;36:1315-1327.
13. Fariss MW, Chan CB, Patel M, Van Houten B, Orrenius S. Role of mitochondria in toxic oxidative stress. *Mol Intervent*. 2005;5:94-111.
14. van der Ploeg AT, Reuser AJ. Pompe's disease. *Lancet (London, England)*. 2008;372:1342-1353.
15. Raben N, Plotz P, Byrne BJ. Acid alpha-glucosidase deficiency (glycogenosis type II, Pompe disease). *Curr Mol Med*. 2002;2:145-166.
16. Shimada Y, Nishimura E, Hoshina H, et al. Proteasome Inhibitor Bortezomib Enhances the Activity of Multiple Mutant Forms of Lysosomal alpha-Glucosidase in Pompe Disease. *JIMD reports*. 2015;18:33-39.
17. Suzuki M, Kondo S, Pei Z, Maekawa A, Saito I, Kanegae Y. Preferable sites and orientations of transgene inserted in the adenovirus vector genome: The E3 site may be unfavorable for transgene position. *Gene Ther*. 2015;22:421-429.
18. Fukuda H, Terashima M, Koshikawa M, Kanegae Y, Saito I. Possible mechanism of adenovirus generation from a cloned viral genome tagged with nucleotides at its ends. *Microbiol Immunol*. 2006;50:643-654.
19. Kanegae Y, Makimura M, Saito I. A simple and efficient method for purification of infectious recombinant adenovirus. *Jpn J Med Sci Biol*. 1994;47:157-166.
20. Pei Z, Shi G, Kondo S, et al. Adenovirus vectors lacking virus-associated RNA expression enhance shRNA activity to suppress hepatitis C virus replication. *Sci Rep*. 2013;3:3575.
21. Pei Z, Kondo S, Kanegae Y, Saito I. Copy number of adenoviral vector genome transduced into target cells can be measured using quantitative PCR: application to vector titration. *Biochem Biophys Res Comm*. 2012;417:945-950.
22. Yamano K, Matsuda N, Tanaka K. The ubiquitin signal and autophagy: an orchestrated dance leading to mitochondrial degradation. *EMBO Rep*. 2016;17:300-316.
23. Nguyen TN, Padman BS, Lazarou M. Deciphering the Molecular Signals of PINK1/Parkin Mitophagy. *Trends Cell Biol*. 2016;26:733-744.
24. Choi KS. Autophagy and cancer. *Exp Mol Med*. 2012;44:109-120.
25. Takamura A, Komatsu M, Hara T, et al. Autophagy-deficient mice develop multiple liver tumors. *Genes Dev*. 2011;25:795-800.
26. Rosenfeldt MT, O'Prey J, Morton JP, et al. p53 status determines the role of autophagy in pancreatic tumour development. *Nature*. 2013;504:296-300.
27. Rao S, Tortola L, Perlot T, et al. A dual role for autophagy in a murine model of lung cancer. *Nat Commun*. 2014;5:3056.
28. Strohecker AM, Guo JY, Karsli-Uzunbas G, et al. Autophagy sustains mitochondrial glutamine metabolism and growth of BrafV600E-driven lung tumors. *Cancer Discov*. 2013;3:1272-1285.
29. Wei H, Wei S, Gan B, Peng X, Zou W, Guan JL. Suppression of autophagy by FIP200 deletion inhibits mammary tumorigenesis. *Genes Dev*. 2011;25:1510-1527.

30. Fu Z, Cheng X, Kuang J, et al. CQ sensitizes human pancreatic cancer cells to gemcitabine through the lysosomal apoptotic pathway via reactive oxygen species. *Mol Oncol*. 2018;12:529-544.
31. Fu D, Zhou J, Zhu WS, et al. Imaging the intracellular distribution of tyrosine kinase inhibitors in living cells with quantitative hyperspectral stimulated Raman scattering. *Nat Chem*. 2014;6:614-622.
32. Kimura T, Takabatake Y, Takahashi A, Isaka Y. Chloroquine in cancer therapy: a double-edged sword of autophagy. *Cancer Res*. 2013;73:3-7.
33. Karasic TB, O'Hara MH, Loaiza-Bonilla A, et al. Effect of gemcitabine and nab-paclitaxel with or without hydroxychloroquine on patients with advanced pancreatic cancer: a phase 2 randomized clinical trial. *JAMA Oncology*. 2019;5:993-998.
34. Zhitomirsky B, Assaraf YG. Lysosomes as mediators of drug resistance in cancer. *Drug Resist Updat*. 2016;24:23-33.
35. Kallunki T, Olsen OD, Jaattela M. Cancer-associated lysosomal changes: friends or foes? *Oncogene*. 2013;32:1995-2004.
36. Sun K, Guo XL, Zhao QD, et al. Paradoxical role of autophagy in the dysplastic and tumor-forming stages of hepatocarcinoma development in rats. *Cell Death Dis*. 2013;4:e501.
37. Raben N, Wong A, Ralston E, Myerowitz R. Autophagy and mitochondria in Pompe disease: nothing is so new as what has long been forgotten. *Am J Med Gen C, Sem Med Gen*. 2012;160c:13-21.
38. Nunnari J, Suomalainen A. Mitochondria: In sickness and in health. *Cell*. 2012;148:1145-1159.
39. Kanegae Y, Terashima M, Kondo S, et al. High-level expression by tissue/cancer-specific promoter with strict specificity using a single-adenoviral vector. *Nucleic Acids Res*. 2011;39:e7.
40. Chiocca EA. Oncolytic viruses. *Nat Rev Cancer*. 2002;2:938-950.
41. Rahal A, Musher B. Oncolytic viral therapy for pancreatic cancer. *J Surg Oncol*. 2017;116:94-103.
42. Nakai M, Komiya K, Murata M, et al. Expression of pIX gene induced by transgene promoter: possible cause of host immune response in first-generation adenoviral vectors. *Hum Gene Ther*. 2007;18:925-936.
43. Miura Y, Yamasaki S, Davydova J, et al. Infectivity-selective oncolytic adenovirus developed by high-throughput screening of adenovirus-formatted library. *Mol Ther*. 2013;21:139-148.
44. Kawashima T, Kagawa S, Kobayashi N, et al. Telomerase-specific replication-selective virotherapy for human cancer. *Clin Cancer Res*. 2004;10:285-292.
45. Fujiwara T, Kagawa S, Kishimoto H, et al. Enhanced antitumor efficacy of telomerase-selective oncolytic adenoviral agent OBP-401 with docetaxel: preclinical evaluation of chemovirotherapy. *Int J Cancer*. 2006;119:432-440.

SUPPORTING INFORMATION

Additional supporting information may be found online in the Supporting Information section.

How to cite this article: Hamura R, Shirai Y, Shimada Y, et al. Suppression of lysosomal acid alpha-glucosidase impacts the modulation of transcription factor EB translocation in pancreatic cancer. *Cancer Sci*. 2021;00:1–14. https://doi.org/10.1111/cas.14921